J. Mol. Chem., 2021, 1(1), 104 Article

JOURNAL OF
MOLECULAR CHEMISTRY

In silico screening of phenolic acids as potential inhibitors of SARS-CoV-2 RNA-dependent RNA polymerase

Bui Thanh Tung*, Nguyen Bao Kim, Phan Hong Minh

VNU University of Medicine and Pharmacy, Vietnam National University, Hanoi, Vietnam.

Received Date: 30-Jan-2021 Accepted and Published on: 16-Feb-2021

ABSTRACT

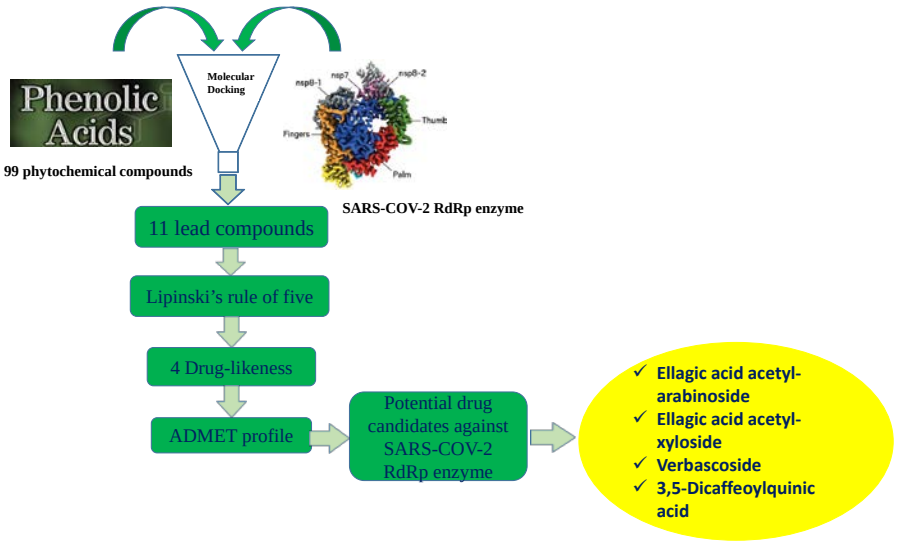

A serious public health concern is the Covid-19 pandemic that causes the acute respiratory syndrome. Thus far, Covid-19's special medicines are indeed an unparalleled obstacle for mankind. It is very essential now to find medications that can cure this disease. As a promising therapeutic target for SARS-COV-2 infection inhibition, the SARS-COV-2 RNA-dependent RNA polymerase (RdRp) enzyme regulating viral replication has been evaluated. This research evaluated the potential of bioactive inhibitors of RNA-dependent RNA polymerase through molecular docking in silico model. Based on the Phenol-Explorer database, we have collected 99 bioactive compounds of the phenolic acids group and compared to remdesivir, which has inhibitory activity with this protein target. 26/99 compounds that had a higher ability to inhibit the SARS-COV-2 RdRp enzyme than remdesivir were further docked targeting the active sites of SARS-CoV-2, as well as SARS-CoV and HCV RdRp. Next, 11 phytochemicals were selected through good binding energy. Predictive druglikeness and ADME/tox filtering tests were further subjected to the top docked compounds. It is suggested that four phytochemicals, namely Ellagic acid acetyl-arabinoside, Ellagic acid acetyl-xyloside, Verbascoside, and 3,5-Dicaffeoylquinic acid, have good pharmacokinetic properties, which may be further explored as anti-SARS-COV-2 agents.

Keywords: SARS-COV-2, RNA-dependent RNA polymerase (RdRp), Molecular docking

INTRODUCTION

Since Covid-19 acute respiratory syndrome was first discovered in Wuhan city, Hubei province, China, the scientific community as well as the entire human race has to face an unprecedented challenge to find the treatment for this disease. With its rapid spread, until January 20th, 2021, there have been 94,963,847 reported cases and 2.050.857 deaths globally (WHO 2020). In Vietnam, 1540 cases and 35 deaths have been reported.[1] One of the concerns is that the symptoms of the disease are often very diverse even can manifest differently in each patient. Clinical symptoms are usually noticed 5 or 6 days after infection but the incubation period can be up to 14 days.[2] Fever, coughing, and fatigue are among the most common symptoms.

SARS-COV-2 has a 29.9 kb-size positive-sense RNA genome. It is composed of 14 open reading frames (ORFs), which encodes for a total of 27 proteins divided into structural and non-structural proteins (NSPs).[3] RNA-dependent RNA polymerase (RdRp) is an important enzyme to the viral RNA life cycle, involved in the

*Corresponding Author: Dr. Bui Thanh Tung
Email: tungasia82@gmail.com

transcription and translation of all RNA virus.[4] The viral RdRps are highly conserved and share typical structural characteristics throughout various species of positive-sense RNA viruses, such as Coronaviruses and Hepatitis C Virus, typical structural characteristics.[5-8] Therefore, RdRp is considered to be a major target for antiviral inhibitors treating Coronaviruses, Dengue virus, Hepatitis C, and Zika.[9-12]

Molecular docking is a modeling technique to predict the position and favorable configuration that a substrate molecule (ligand) can bind to a protein molecule (target). This *in silico* method saves much time and costs in the screening of compounds compared with the experimental methods.[13]

The rapid spread of Covid-19 has globally emphasized the development of coronavirus vaccines and therapies need. Therefore, we have investigated to find a potential drug to inhibit RNA-dependent RNA polymerase (RdRp) for Covid-19 treatment.

Because of the minimal side effects and effective health benefits, plant-based anti-infection therapies are attracting the attention of modern world healthcare researchers.[14] In recent years, the development of plant-based drugs has been continuously examined for their antibacterial, antiviral, anticancer, and antioxidant activities.[15,16] Plant-based potential bioactive compounds with antiviral properties have been shown to be superior and can be associated with pre-existing treatments and various delivery strategies to increase antiviral efficacy along with good bioavailability.[17-19]. Moreover, many studies revealed that several antiviral plants have shown promising therapeutic potential against SARS-CoV and SARS-CoV-2, hence phytomedicine has efficacy against COVID-19.[20-22] Our research focused on the virtual screening against SARS-CoV-2 and related RNA-dependent RNA polymerase viruses of phenolic acids derived from usual foods and medicinal plants. Phenolic compounds were also reported about antiviral properties against various viruses.[23-26]

MATERIAL AND METHOD

Retrieval and preparation of protein structure

The three-dimensional (3D) of SARS-CoV-2 RdRp (PDB ID: 6M71), SARS-CoV RdRp (PDB ID: 6NUR) and HCV RdRp (PDB ID: 4WTG) were retrieved from the Protein Data Bank RCSB.[27-29] All water molecules and co-crystal were removed from the protein molecule using Discovery Studio Visualizer 4.0 software while missing hydrogen atoms were added using Autodock Vina before regenerating the active site using MGL Autodock tools 1.5.6 software. The protein is then saved in pdbqt format to prepare for the docking program. During the docking, the two active site aspartations (ASP760 and ASP761) were viewed as flexible.

Ligands preparation

The ligand structures were collected from Phenol-Explorer for the RNA-dependent RNA polymerase enzyme (RdRp) target involved 99 bioactive compounds. The structures were downloaded from Phenol-Explorer in Smiles format and then converted into 3D structures in PDB format using MOE software.[30] Structure Data Format (SDF) structures of the reference inhibitors (Remdesivir) were retrieved from the PubChem database.[31] After that, they were optimized by Avogadro software using Conjugate Gradients and converted to pdbqt format using Autodock Tools software.

Molecular docking study

AutoDock Vina performed an initial simulated screening of 99 bioactive compounds against SARS-CoV-2 RdRp (PDB ID: 6M71). Different binding conformations around the active grid box size (30 Å x 30 Å x 30 Å) was located by using a larger grid box size of (60 Å x 60 Å x 60 Å). Compounds with higher binding affinities and conformational poses that were docked into the active side region were chosen for further analysis from the initial docking analysis.

A hit-list of the top 26 ranking compounds with binding affinities higher than the reference inhibitors was established based on the docking ratings, binding poses and catalytic residue interaction, and the top eleven compounds were selected from this list. The compounds were further docked at the active SARS-CoV-2, SARS-CoV, and Hepatitis C Virus (HCV) RdRp sites using the Autodock vina. The active region of the SARS-CoV-2 RdRp defined by a grid box size of 30 Å x 30 Å x 30 Å centered at (x, y, z) of (121, 120, 125) A˚ was used for docking [32]. With Discovery Studio Visualizer 2020, the molecular interactions between proteins and selected compounds with higher binding affinity to proteins were viewed.

Lipinski's rule of five

Lipinski rule of five helps to compare drug-like and non-drug-like molecules [33]. Lipinski's rule of five is popularly used to evaluate the potential molecular to become a therapeutical drug. This rule acts as a filter to screen promising compounds with a particular pharmacological activity.

We used the online tool to evaluate Lipinski's rule of five.[34] The chemical structures were downloaded from the Pubchem database and set at pH 7.0.[35]

Prediction of ADMET by computational analysis

In order to analyze the physiochemical efficiency of five above-mentioned drugs to inhibit the target protein, we used in silico ADMET profiling. ADMET profile involves five parameters: absorption, distribution, metabolism, excretion and toxicity that play a significant role to demonstrate the likelihood of success of a drug. Drug absorption depends on factors including membrane permeability, intestinal absorption, levels of skin permeability, substrate or inhibitor of P-glycoprotein. Drug distribution relies on factors like blood-brain barrier (logBB), CNS permeability, and volume of distribution (VDss). Based on the CYP models for substrate or inhibition (CYP2D6, CYP3A4, CYP1A2, CYP2C19, CYP2C9, CYP2D6, and CYP3A4), metabolism is expected. Based on the total clearance model and the renal OCT2 substrate, excretion is expected. Based on AMES toxicity, hERG inhibition, hepatotoxicity, and skin sensitization, the toxicity of drugs is expected. These criteria have been determined and their standard ranges have been tested for compliance. ADMET profiling was predicted using the pkCSM tool.[36] The canonical SMILES molecular structures of collected compounds were retrieved from Pubchem.[31]

RESULTS

Binding pocket

Using the MOE SiteFinder to find the RdRp binding pocket, we found these essential acid amine: ASP760, ASP761, ASP623, ASP452, TYR455, TYR456, ARG553, PRO620, ARG624, GLU811, TYR619, PRO620, LYS621, CYS622, ASP623, SER681, LYS798, GLU811, SER814 were involved in the active site.

Figure 1 illustrates the active site or binding pocket of SARS-CoV-2 RdRp in the yellow box

Figure 1: The binding pocket of SARS-COV-2 RdRp

Molecular docking of compounds with the target protein

After preparing the ligands, we docked 99 bioactive compounds retrieved with RNA-dependent RNA polymerase enzyme to screen target inhibitory activity. The results are shown in Table 1.

Table 1: The docking results of 99 phytochemicals and reference compound with RNA-dependent RNA polymerase enzyme

No	Name	Binding Energy With Rdrp Enzyme (Kcal/Mol)	No	Name	Binding Energy With Rdrp Enzyme (Kcal/Mol)
1	2,3-Dihydroxybenzoic acid	-5.8	51	5-8'-Dehydrodiferulic acid	-7.4
2	2,4-Dihydroxybenzoic acid	-5.2	**52**	**Chlorogenic acid**	**-8**
3	2,6-Dihydroxybenzoic acid	-5.5	53	5-Feruloylquinic acid	-7.4
4	2-Hydroxybenzoic acid	-5.2	**54**	**5-p-Coumaroylquinic acid**	**-7.7**
5	3,5-Dihydroxybenzoic acid	-5.4	55	8-O-4'-Dehydrodiferulic acid	-7.1
6	3-Hydroxybenzoic acid	-5.1	56	Avenanthramide 2c	-7.4
7	4-Hydroxybenzoic acid	-4.9	57	Avenanthramide 2f	-6.4
8	4-Hydroxybenzoic acid 4-O-glucoside	-6.3	58	Avenanthramide 2p	-6.9
9	5-O-Galloylquinic acid	-6.8	**59**	**Avenanthramide K**	**-7.6**
10	Benzoic acid	-4.6	60	Caffeic acid	-5.9
11	**Ellagic acid**	**-8.2**	61	Caffeic acid 4-O-glucoside	-7.2
12	**Ellagic acid acetyl-arabinoside**	**-9**	62	Caffeic acid ethyl ester	-5.2
13	**Ellagic acid acetyl-xyloside**	**-8.5**	63	Caffeoyl aspartic acid	-6.6
14	**Ellagic acid arabinoside**	**-8.9**	64	Caffeoyl glucose	-6.4
15	Ellagic acid glucoside	-5.9	65	Caffeoyl tartaric acid	-7.5
16	Gallic acid	-5.9	66	Chicoric acid	-7.4
17	**Gallic acid 3-O-gallate**	**-8.5**	67	Sinapine	-6
18	Gallic acid 4-O-glucoside	-6.7	68	Cinnamoyl glucose	-6.7
19	Gallic acid ethyl ester	-5.5	69	Ferulic acid	-5.4
20	Galloyl glucose	-7.4	70	Ferulic acid 4-O-glucoside	-6.6
21	Gentisic acid	-5.4	71	Feruloyl glucose	-7.4
22	veratric acid	-4.9	72	Feruloyl tartaric acid	-7.5
23	Protocatechuic acid	-5.7	73	Hydroxycaffeic acid	-5.7
24	Protocatechuic acid 4-O-glucoside	-6.9	74	Isoferulic acid	-5.6
25	syringealdehyde	-4.9	75	m-Coumaric acid	-5.4
26	Vanillin	-4.9	76	o-Coumaric acid	-5.4
27	Syringic acid	-5.4	77	p-Coumaric acid	-5.2
28	**Valoneic acid dilactone**	**-8.6**	78	p-Coumaric acid 4-O-glucoside	-6.7
29	Vanillic acid	-5	79	p-Coumaric acid ethyl ester	-5.5
30	Acetosyringone	-5.2	80	p-Coumaroyl glucose	-6.7
31	**1,2-Diferuloylgentiobiose**	**-8.3**	81	p-Coumaroyl glycolic acid	-6.2
32	1,2-Disinapoylgentiobiose	-5	82	p-Coumaroyl malic acid	-6.9
33	**24-Methylcholestanol ferulate**	**-7.8**	83	p-Coumaroyl tartaric acid	-6.8
34	**24-Methylcholesterol ferulate**	**-8.6**	84	p-Coumaroyl tartaric acid glucosidic ester	-5.1
35	**24-Methylenecholestanol ferulate**	**-7.8**	85	p-Coumaroyl tyrosine	-6.8
36	**24-Methyllathosterol ferulate**	**-7.6**	**86**	**p-Coumaroylquinic acid**	**-7.8**
37	**3,4-Dicaffeoylquinic acid**	**-8.8**	87	Rosmarinic acid	-6.9
38	3,4-Diferuloylquinic acid	-7.5	88	Sinapic acid	-5.3
39	**3,5-Dicaffeoylquinic acid**	**-9**	89	Chicoric acid	-5.5

40	**3,5-Diferuloylquinic acid**	**-8.6**	**90**	**Sitosterol ferulate**	**-8**
41	**3-Caffeoylquinic acid**	**-8.1**	**91**	**Stigmastanol ferulate**	**-7.9**
42	**3-Feruloylquinic acid**	**-7.7**	**92**	**Verbascoside**	**-8.6**
43	3-p-Coumaroylquinic acid	-6.8	93	3,4-Dihydroxyphenylacetic acid	-5.1
44	**3-Sinapoylquinic acid**	**-8.6**	94	4-Hydroxyphenylacetic acid	-4.8
45	**4,5-Dicaffeoylquinic acid**	**-8.2**	95	Homovanillic acid	-5.1
46	4-Caffeoylquinic acid	-7.1	96	Homoveratric acid	-4.9
47	**4-Feruloylquinic acid**	**-7.8**	97	Methoxyphenylacetic acid	-5
48	4-p-Coumaroylquinic acid	-7.4	98	Dihydro-p-coumaric acid	-5.1
49	4-Sinapoylquinic acid	-7.3	99	Dihydrocaffeic acid	-5.3
50	5-5'-Dehydrodiferulic acid	-6.9	100	Remdesivir	-7.4

Remesdevir is an antiviral drug that has been approved by the FDA for the treatment of Covid-19 requiring hospitalization [37]. As an RNA polymerase (RdRp) inhibitor, it can inhibit coronavirus replication in respiratory epithelial cells [38]. Therefore, in this study, we compared the docking scores of the ligands with remesdevir to evaluate the compounds' abilities to inhibit RNA-dependent RNA polymerase enzyme. Remdesivir and the reference inhibitor had binding affinities of –7.6 Kcal/mol for the RdRp of SARS-CoV-2. Elfiky et al also reported the -7.6 (kcal/mol) binding affinities with the SARS-COV-2 RdRp target [6]. Figure 2 shows the interaction between remdesivir and the RdRp enzyme.

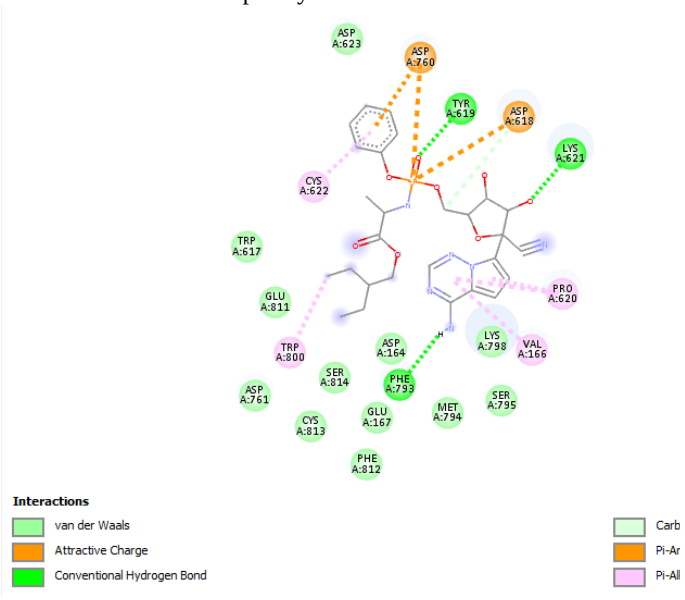

Figure 2: Interaction between remdesivir and RdRp enzyme

A hit list of 26 bioactive compounds was defined based on the negative and low value of ΔG and compared with the reference inhibitor (Table 1). These top compounds, which include compound categories of caffeic acid, chlorogenic acid, and ferulic acid, display binding energy ranging from -9 to -7.6 Kcal/mol. From these, 26 bioactive compounds were further docked at the active SARS-CoV-2, SARS-CoV, and Hepatitis C Virus (HCV) RdRp sites. The results were shown in table 2.

Table 2: Binding energy of 26 selected-compounds at the active site of SARS-CoV-2, SARS-CoV, and Hepatitis C Virus (HCV) RdRp

No	Compounds	Binding energy with SARS-CoV-2 RdRp (Kcal/mol)	Binding energy with SARS-CoV RdRp (Kcal/mol)	Binding energy with HCV RdRp (Kcal/mol)
1	Ellagic acid	-7	-8.1	-7.8
2	**Ellagic acid acetyl-arabinoside**	**-9**	**-8.2**	**-8**
3	**Ellagic acid acetyl-xyloside**	**-8.9**	**-8.6**	**-8.4**
4	**Ellagic acid arabinoside**	**-7.9**	**-7.6**	**-8.4**
5	**Gallic acid 3-O-gallate**	**-7.9**	**-7**	**-8.1**
6	**Valoneic acid dilactone**	**-8**	**-7.2**	**-7.3**
7	**1,2-Diferuloylgentiobiose**	**-8.1**	**-7.1**	**-7.3**
8	24-Methylcholestanol ferulate	-6.4	-7.9	-6.9
9	24-Methylcholesterol ferulate	-7.5	-7.3	-8
10	24-Methylenecholestanol ferulate	-7.4	-7	-7.3
11	24-Methyllathosterol ferulate	-7.2	-7.3	-7
12	**3,4-Dicaffeoylquinic acid**	**-8.3**	**-8**	**-7.5**
13	**3,5-Dicaffeoylquinic acid**	**-9.2**	**-8.4**	**-8.2**
14	**3,5-Diferuloylquinic acid**	**-8.1**	**-7.1**	**-7.8**
15	3-Caffeoylquinic acid	-6.7	-7.3	-7.2
16	3-Feruloylquinic acid	-7	-7.1	-7
17	**3-Sinapoylquinic acid**	**-7.8**	**-7.6**	**-8.8**
18	4,5-Dicaffeoylquinic acid	-7.2	-7.3	-7.3
19	4-Feruloylquinic acid	-7	-7.2	-6.7
20	Chlorogenic acid	-7.1	-7.2	-7.2
21	5-p-Coumaroylquinic acid	-6.8	-6.9	-6.9
22	Avenanthramide K	-6.8	-6.7	-6.9
23	p-Coumaroylquinic acid	-6.8	-7.1	-6.9

24	Sitosterol ferulate	-7.6	-7.5	-7.4
25	Stigmastanol ferulate	-7.7	-7.4	-7.5
26	**Verbascoside**	**-8.4**	**-8.5**	**-8.4**

From table 2, the best eleven docked compounds were chosen by docking these selected compounds with the active region of SARS-CoV-2, as well as SARS-CoV and HCV. They are Ellagic acid acetyl-arabinoside (C1), Ellagic acid acetyl-xyloside (C2), Verbascoside (C3), 3,5-Dicaffeoylquinic acid (C4), Gallic acid 3-O-gallate(C5), 1,2-Diferuloylgentiobiose (C6), 3,4-Dicaffeoylquinic acid (C7), 3,5-Diferuloylquinic acid (C8), 3-Sinapoylquinic acid (C9), Valoneic acid dilactone (C10), and Ellagic acid arabinoside (C11). Binding energy of these eleven compounds and the reference compound to the active site residues of viral RNA dependent RNA polymerase were shown in figure 3.

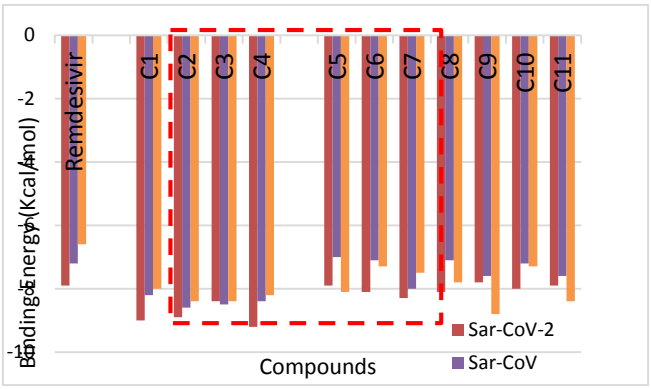

Figure 3: Binding energy of top eleven phytochemicals and reference compound to the active site residues of viral RNA-dependent RNA polymerase. The red dotted line shows the top 4 docked phenolic acids

As shown by the docking ratings, these compounds, which belong to the phytochemical groups of phenolic acids (Table 3), can bind to the three active site domains of the viral RdRp with good binding energy.

Table 3: Top eleven phytochemicals with the active site residues of SAR CoV-2 RNA-dependent RNA polymerase

Compounds	Structure	Plant Source
Remdesivir	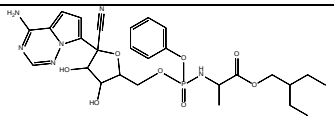	
Ellagic acid acetyl-arabinoside (C1)	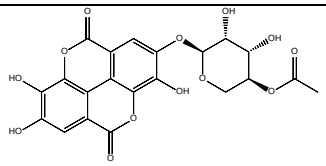	*Rubus idaeus* (Juglandaceae)
Ellagic acid acetyl-xyloside (C2)	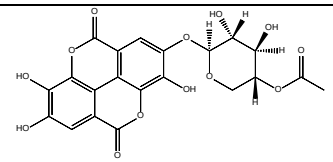	*Rubus idaeus* (Juglandaceae)
Verbascoside (C3)	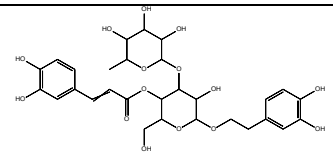	*Verbena officinalis* (Verbenaceae)
3,5-Dicaffeoylquinic acid (C4)	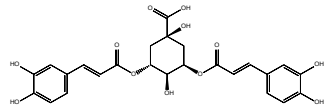	*Laggera alata* (Asteraceae) *Lonicera japonica* *Ilex kaushue*
Gallic acid 3-O-gallate (C5)	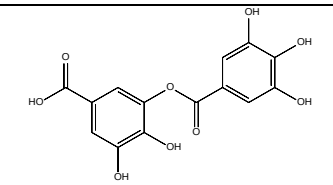	*Terminalia chebula*
1,2-Diferuloylgentiobiose (C6)	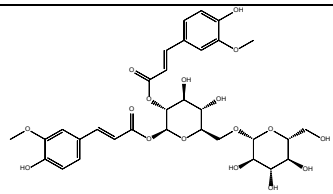	*Brassica oleracea* (Brassicaceae)
3,4-Dicaffeoylquinic acid (C7)	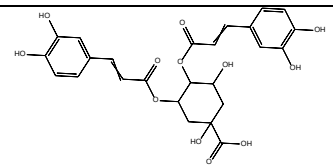	Coffea (Rubiaceae)
3,5-Diferuloylquinic acid (C8)	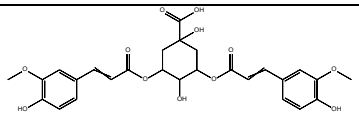	*Daucus carota* (Apiaceae)
3-Sinapoylquinic acid (C9)	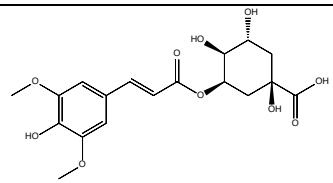	*Coffea canephora* (Rubiaceae)
Valoneic acid dilactone (C10)	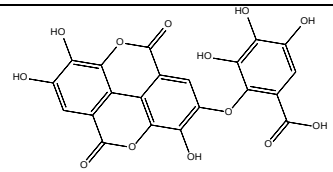	*Juglans regia* (Juglandaceae)
Ellagic acid arabinoside (C11)	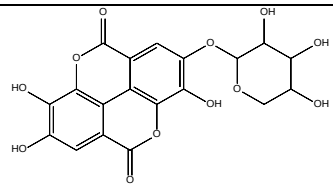	*Rubus idaeus* (Juglandaceae)

The 4 top bioactive compounds docked into the active site of SARS-CoV-2 RdRp are Ellagic acid acetyl-arabinoside, Ellagic acid acetyl-xyloside, Verbascoside, and 3,5-Dicaffeoylquinic acid. It was observed that all these compounds were the topmost docked compound to the RdRp of all three SARS-CoV-2, SARS-CoV and HCV (Figure 4).

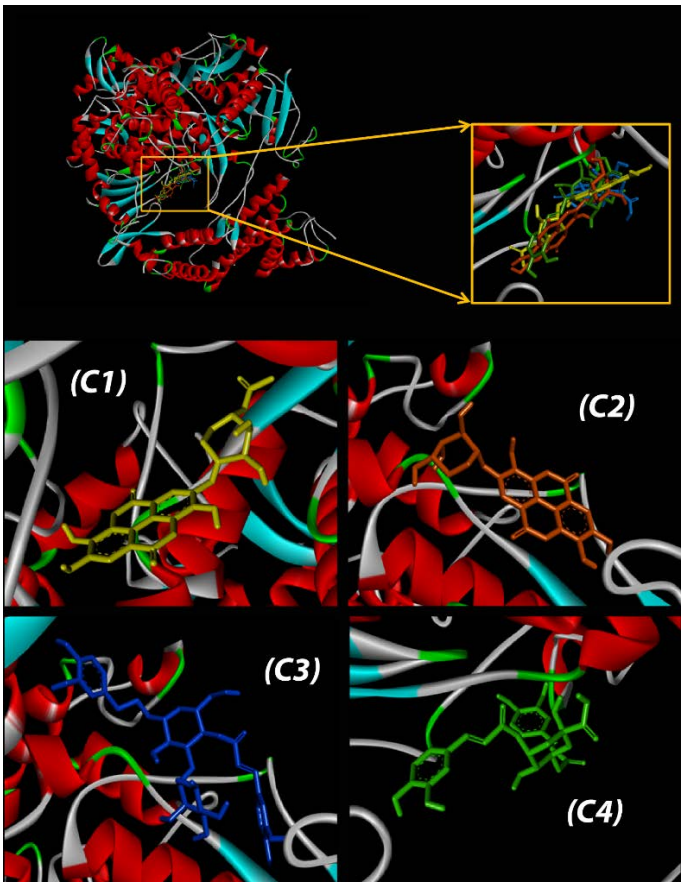

Figure 4: The top 4 bioactive compounds Ellagic acid acetyl-arabinoside (C1) (yellow), Ellagic acid acetyl-xyloside (C2) (orange), Verbascoside (C3) (blue), and 3,5-Dicaffeoylquinic acid (C4) (green) docked into the active site of SARS-CoV-2 RdRp

Molecular interactions between the selected phytochemicals and viral RdRps

Ligand-amino acid interactions of these 4 compounds viral RdRp are shown in Table 4. It is revealed that the ligands majorly interacted with the residues through hydrogen bonds and π-anion bonds. SARS-CoV-2 and HCV RdRps active site residues interacting with the topmost binding compounds are seen in Table 4 and Figure 5.

Table 4. Molecular interactions between the selected phytochemicals and viral RdRps

Compounds	Viral RdRp	Hydrogen bonds	π-anion bonds	Other interactions
Ellagic acid acetyl-arabinoside	SARS-CoV-2	**ASP760**, ASP623, ARG553, LYS621, TYR619, TRP800	ASP623, ARG553	
Ellagic acid acetyl-xyloside		**ASP760**, LYS621, TYR622, CYS622, GLU811,	ASP618, GLU811	LYS798
Verbascoside		**ASP760**, LYS621, LYS551, CYS813	ARG553, GLU811	ARG624
3,5-Dicaffeoylquinic acid		LYS621, TYR619, SER814, PHE793	**ASP761**	PRO620, CYS622, SER795
Ellagic acid acetyl-arabinoside	SAR-CoV	ARG553, ARG624, ARG555, THR556, MET542, SER682	ASP623	
Ellagic acid acetyl-xyloside		LYS621, ASP452, TYR455, ASP760	ARG553	
Verbascoside		ARG553, ASP452, THR556, ARG624	ASP623, ARG624	LYS621
3,5-Dicaffeoylquinic acid		ASP760, ARG624, LYS621, TRP617	ARG553, ASP761	TYR455
Ellagic acid acetyl-arabinoside	HCV	ASP225, SER282, SER288	ARG158, ASP318	
Ellagic acid acetyl-xyloside		ASP225, PHE224, ASN291	ARG158, ASP318	
Verbascoside		ASN291, ASP319, ASP318, ASP225	ARG158	HIS223
3,5-Dicaffeoylquinic acid		ARG158, ASN291, PHE224, ASP319	ASP220	

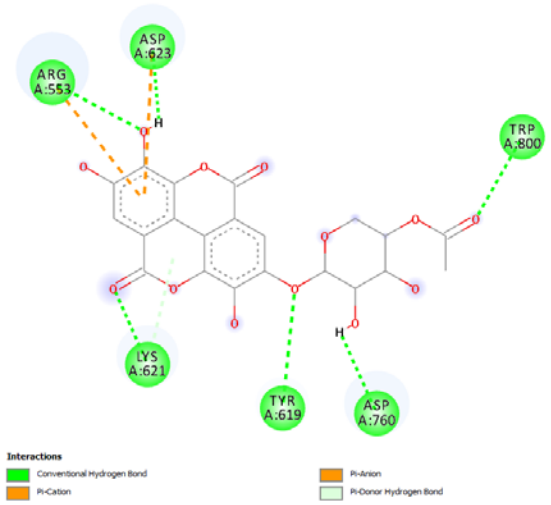

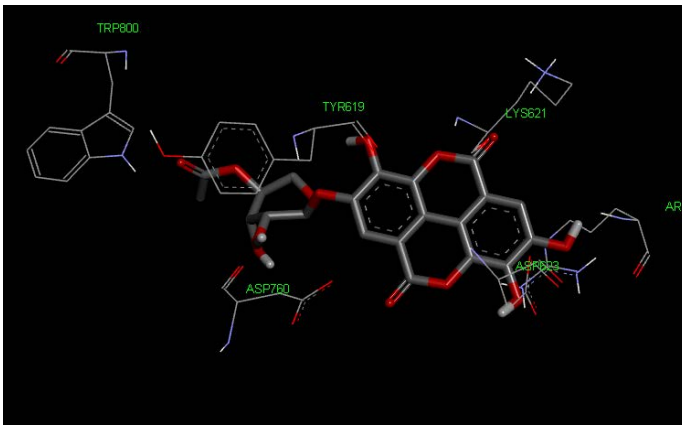

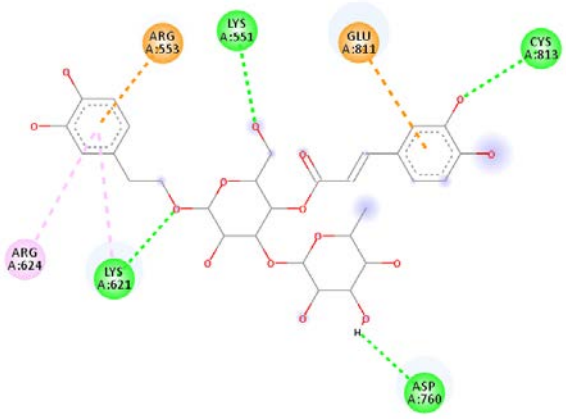

Ellagic acid acetyl-arabinoside (C1)

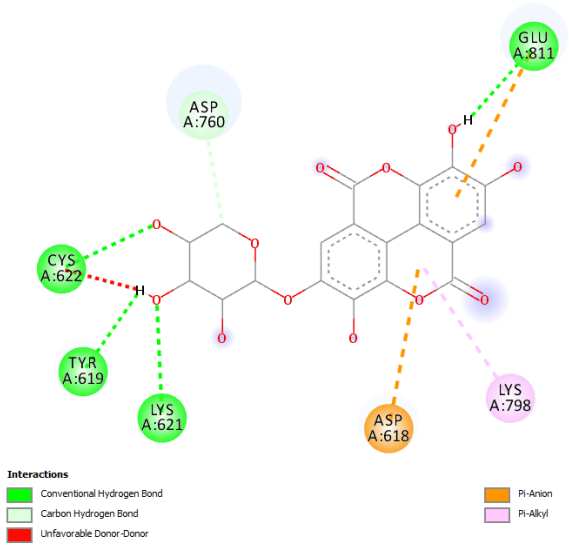

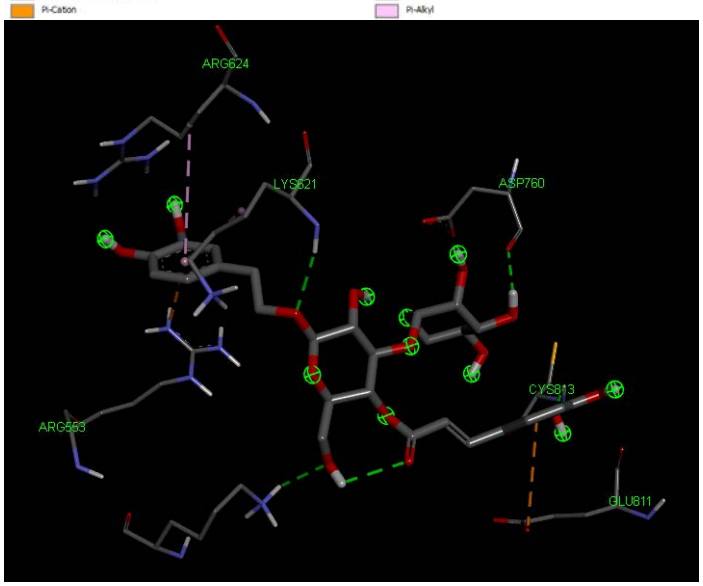

Verbascoside (C3)

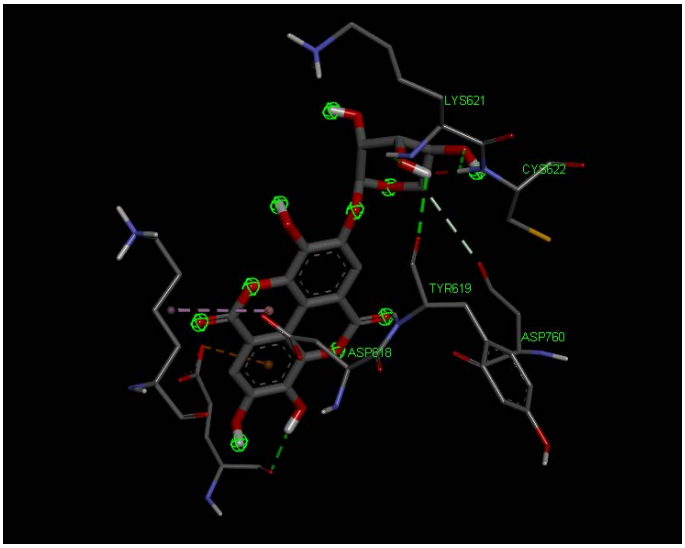

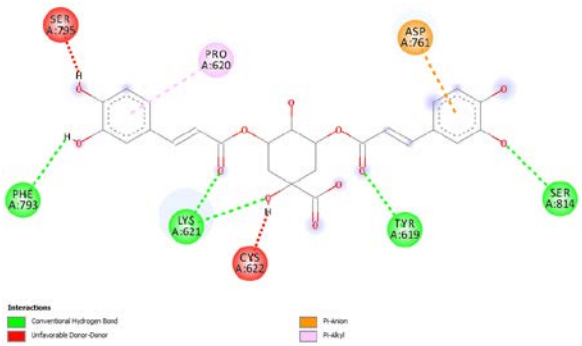

Ellagic acid acetyl-xyloside (C2)

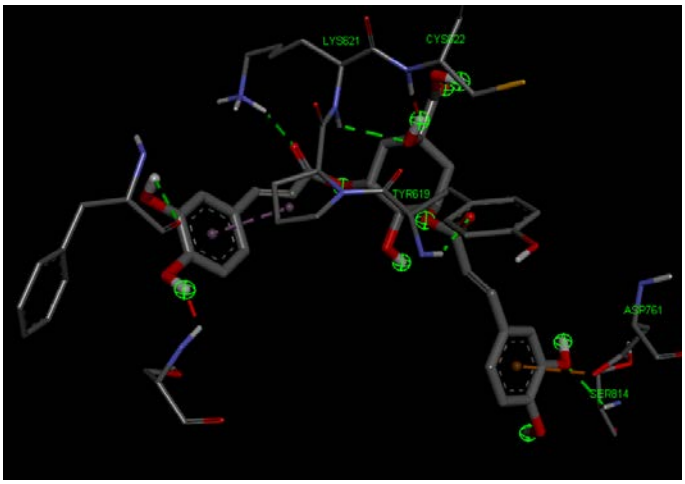

3,5-Dicaffeoylquinic acid (C4)

Figure 5: The interaction views of the best four compounds Ellagic acid acetyl-arabinoside, Ellagic acid acetyl-xyloside, Verbascoside, and 3,5-Dicaffeoylquinic acid against the active site of SARS-CoV-2 RdRp. The green dashed lines reflect hydrogen bonds, while π-anion bonds are represented in dashed-orange lines.

3,5-Dicaffeoylquinic acid, as known as isochlorogenic acid A, which had the lowest binding energy to SARS-CoV-2, was docked into the active site of the enzyme in a similar manner to remdesivir. This compound was observed to interact via conventional hydrogen bond to LYS624, TYR619, SER814,PHE793; π-anion electrostatic bond with ASP761. 3,5-Dicaffeoylquinic acid showed the highly binding pattern with both SARS-CoV and HCV since it also docked via multiple non-covalent interactions to the active region of SARS-CoV and HCV RdRp. Ellagic acid acetyl-arabinoside, a Hydroxybenzoic acids, also interacted to SARS-CoV-2, SARS-CoV and HCV with a conserved binding pattern. It was found that this compound interacts with conventional hydrogen bonding to almost amino acids, namely ASP760, ASP623, ARG553, LYS621, TYR619, TRP800. Ellagic acid acetyl-xyloside and Verbascoside had high binding energies to the viral RdRp through some same amino acids, such as hydrogen bonds with ASP760, LYS621; π-anion electrostatic bond with GLU811.

Lipinski's rule of five

Lipinski's rule of five helps in distinguishing between drug-like and non-drug-like molecules. It predicts high probabilities of drug-like effectiveness or failure for molecules complying with 2 or more of the following rules: molecular mass (MW) below 500 Dalton; high lipophilicity (expressed as LogP below 5); less than 5 donors of hydrogen bonds (HBD); less than 10 acceptors of hydrogen bonds (HBA1); molar refractivity (MR) should be between 40-130.

All these top-compounds are satisfied with more than 2 criteria. Then, we focus on analyzing the pharmacokinetic properties including absorption, distribution, metabolism, excretion and toxicity of these drugs.

Table 5: The result of Lipinski's rule of five

No	Drugs	Molecular weight	HBD	HBA1	logP	MR	Drug-ikeness
1	Ellagic acid acetyl-arabinoside	476.9	5	13	-1.525850	100.778465	Yes
2	Ellagic acid acetyl-xyloside	434.0	6	12	-2.286659	90.570259	Yes
3	Verbascoside	624.0	9	15	-1.015900	127.095245	Yes
4	3,5-Dicaffeoyl quinic acid	516.0	7	12	1.029601	125.197540	Yes

Prediction of absorption, distribution, metabolism, excretion and toxicity (ADMET) profile

The prediction of absorption, distribution, metabolism, excretion and toxicity profile of five selected drugs were shown in Table 6.

Table 6. The result of ADMET profile

Properties	Ellagic acid acetyl-arabinoside	Ellagic acid acetyl-xyloside	Verbascoside	3,5-Dicaffeoylquinic acid
Absorption				
Water solubility (log mol/L)	-3.157	-3.172	-2.906	-2.952
Caco2 permeability (log Papp in 10^{-6} cm/s)	0.783	0.783	0.096	-1.147
Intestinal absorption (human) (% Absorbed)	57.85	60.754	32.119	44.225
Distribution				
VDss (human) (log L/kg)	0.542	0.542	2.255	1.7
Fraction unbound (human) (Fu)	0.067	0.062	0.269	0.28
BBB permeability	-1.656	-1.759	-1.86	-2.069
Metabolism				
CYP2D6 substrate	No	No	No	No
CYP3A4 substrate	No	No	No	Yes
CYP2D6 inhibitor	No	No	No	No
CYP3A4 inhibitor	No	No	No	No
Excretion				
Total Clearance (log ml/min/kg)	0.734	0.738	0.479	-0.044
Toxicity				
AMES toxicity	No	No	No	No
Hepatotoxicity	No	No	No	No
Skin Sensitization	No	No	No	No

DISCUSSION

An integral component of the international response to the COVID-19 pandemic is the development of the potential of plant chemicals. In this study, phytochemicals are identified as possible inhibitors of SARS-CoV-2 RdRp from foods and medicinal plants. As this enzyme plays a key role in the machinery for coronaviral replication/transcription, it is considered as an effective target for potential therapies in which lead inhibitors such as remdesivir have been approved by the FDA. Multiple non-covalent interactions with the active RdRp sites of all three SARS-CoV-2, SARS-CoV and HCV were found to be the top four bioactive compounds. These compounds can bind more closely than remdesivir, used in this study as a reference. Hence, these compounds may be able to bind tightly to the new RdRp strain of coronavirus and thus compromise the role of polymerase.

Comparing the interactions of five drugs with remdesivir, we can see that the bonds of five drugs have similarities with remdesivir to Rdrp enzyme. This is demonstrated by their association with several important amino acids such as LYS621, ASP761, ARG553 and specially π-anion bond with ASP760. In addition, these drugs also bind to many other amino acids such as TYR619, PRO620, ASP618, CYS622,… In recent studies, they demonstrated the same residues to bind strongly within active sites of RdRp.[39,40]

The Lipinski and ADMET prediction revealed that the top four docked compounds were non-toxic, drug-like natural compounds bound to the SARS-CoV RdRp active site. The absorption of drugs is predicted based on membrane permeability, intestinal absorption, skin permeability levels, P-glycoprotein substrate or inhibitor. The intestinal absorption (human) percentage of all mentioned compounds is comparatively high/medium: Ellagic acid acetyl-arabinoside (57,85%), Ellagic acid acetyl-xyloside (57.85%), Verbascoside (33.119%), and 3,5-Dicaffeoylquinic acid (44.225%) (A mocule with an absorbance of less than 30% is considered to be poorly absorbed) [40]. The distribution extent is a parameter to signify the distribution of medication in numerous tissues in vivo. VDss is considered low if below 0.71L/kg (log VDss < -0.15) and high if above 2.81 L/kg (log VDss > 0.45) [41]. The results confirmed that the distribution volume of dihydroergotamine and darunavir are high (from 0.542 to 2.255). For a given drug, a log BB < -1 is considered to poorly cross the blood-brain barrier.[41] All four phytochemicals were predicted to difficultly cross the blood-brain barrier. Metabolism is anticipated based at the CYP fashions for substrate or inhibition (CYP2D6, CYP3A4, CYP1A2, CYP2C19, CYP2C9, CYP2D6, and CYP3A4). A significant detoxification enzyme in the body, primarily found in the liver, is cytochrome P450. The two main isoforms of cytochrome P450 responsible for drug metabolism are CYP2D6 and CYP3A4.[42] The results confirm that almost compounds are not substrates as well as inhibitors for the two subtypes, leading to metabolism in the liver. The prediction effects display that the total clearance of Ellagic acid acetyl-xyloside is the best observed by means Ellagic acid acetyl-arabinoside, Verbascoside, and 3,5-Dicaffeoylquinic acid. In terms of toxicity, all four substances have no AMES toxicity, nor are they toxic to the liver or skin.

Parameters that indicate desirable ADME/tox and pharmacokinetic properties were shown by the results of the expected filtering analyses of the five compounds. In addition, this demonstrates the drug-ability potential of the best-docked phenolic acids.

CONCLUSION

Our research revealed that specific phenolic acid compounds from foods and medicinal plants are potential inhibitors of SARS-CoV-2. They are successful in establishing strong and favorable binding affinity with the SARS-CoV-2 RdRp and SARS-CoV and HCV active sites, thereby compromising the catalytic functions of this enzyme. All four compounds above satisfied Lipinski's rule of five rule and have good absorption properties, less toxicity, and drug-like properties. These phytochemicals can provide a wealth of variety in the chemical structure that can assist in the production of therapeutic agents, which prevent SASR-CoV-2 pandemic. In conclusion, based on our findings, we suggest that four promised bioactive compounds should be deeper studied *in vitro*, *in vivo* and in clinical trials to handle this intricate infection.

REFERENCES AND NOTES

1. V. Ministery of Health, Information on acute respiratory infections COVID-19. https://ncov.moh.gov.vn.
2. B.S. Chhikara, B. Rathi, J. Singh, P. FNU. Corona virus SARS-CoV-2 disease COVID-19: Infection, prevention and clinical advances of the prospective chemical drug therapeutics. *Chem. Biol. Lett.* **2020**, 7 (1), 63–72..
3. A. Wu, Y. Peng, B. Huang *et. al*. Genome Composition and Divergence of the Novel Coronavirus (2019-nCoV) Originating in China. **2020**, 27(3), 325-28.
4. J.A. Bruenn. A structural and primary sequence comparison of the viral RNA-dependent RNA polymerases. *Nucleic acids research* **2003**, 31(7), 1821-29.
5. M. Machitani, M. Yasukawa, J. Nakashima *et. al.* RNA-dependent RNA polymerase, RdRP, a promising therapeutic target for cancer and potentially COVID-19. *Cancer Science* **2020**, 111(11), 3976-84.
6. A.A. Elfiky. Ribavirin, Remdesivir, Sofosbuvir, Galidesivir, and Tenofovir against SARS-CoV-2 RNA dependent RNA polymerase (RdRp): A molecular docking study. *Life Sci* **2020**, 253117592-92.
7. M.S.A. Parvez, M.A. Karim, M. Hasan *et. al.* Prediction of potential inhibitors for RNA-dependent RNA polymerase of SARS-CoV-2 using comprehensive drug repurposing and molecular docking approach. *Int J Biol Macromol* **2020**, 1631787-97.
8. A.J. te Velthuis. Common and unique features of viral RNA-dependent polymerases. *Cell Mol Life Sci* **2014**, 71(22), 4403-20.
9. A. Madhvi, S. Hingane, R. Srivastav *et. al.* A screen for novel hepatitis C virus RdRp inhibitor identifies a broad-spectrum antiviral compound. *Scientific Reports* **2017**, 7(1), 5816.
10. J. Yuan, J. Yu, Y. Huang *et. al.* Antibiotic fidaxomicin is an RdRp inhibitor as a potential new therapeutic agent against Zika virus. *BMC Medicine* **2020**, 18(1), 204.
11. A.A. Elfiky. Anti-HCV, nucleotide inhibitors, repurposing against COVID-19. *Life Sci* **2020**, 248117477-77.
12. G. Li, E. De Clercq. Therapeutic options for the 2019 novel coronavirus (2019-nCoV). *Nature reviews. Drug discovery* **2020**, 19(3), 149-50.
13. A. Amberg In Drug Discovery and Evaluation: Safety and Pharmacokinetic Assays, H.G. Vogel, J. Maas, F.J. Hock, D. Mayer, Eds.; Springer Berlin Heidelberg: Berlin, Heidelberg, **2013**, pp 1273-96.
14. R. Ghildiyal, V. Prakash, V.K. Chaudhary *et. al.* In Plant-derived Bioactives, M.K. Swamy, Ed.; Springer Singapore: Singapore, **2020**, pp 279-95.

15. D. Biswas, S. Nandy, A. Mukherjee *et. al*. Moringa oleifera Lam. and derived phytochemicals as promising antiviral agents: A review. *South African Journal of Botany* **2020**, 129272-82.
16. H. Lillehoj, Y. Liu, S. Calsamiglia *et. al.* Phytochemicals as antibiotic alternatives to promote growth and enhance host health. *Veterinary research* **2018**, 49(1), 76.
17. R. Kapoor, B. Sharma, S.S. Kanwar. Antiviral Phytochemicals: An Overview. *Biochemistry & Physiology: Open Access* **2017**, 06(02).
18. R. Ghildiyal, V. Prakash, V.K. Chaudhary *et. al.* Phytochemicals as Antiviral Agents: Recent Updates. *Plant-derived Bioactives* **2020**279-95.
19. K. Ramachandran, M. Akram, U. Laila. Anti-Viral Medicinal Plants & Their Chemical Constituents, Experimental and Clinical Pharmacology of Antiviral Plants. *Science, Technology & Human Values* **2020**, 11-17.
20. L. Zhang, Y. Liu. Potential interventions for novel coronavirus in China: A systematic review. *J Med Virol* **2020**, 92(5), 479-90.
21. J.S. Mani, J.B. Johnson, J.C. Steel *et. al.* Natural product-derived phytochemicals as potential agents against coronaviruses: A review. *Virus Res* **2020**, 284197989-89.
22. J. Lung, Y.-S. Lin, Y.-H. Yang *et. al.* The potential chemical structure of anti-SARS-CoV-2 RNA-dependent RNA polymerase. *J Med Virol* **2020**, 92(6), 693-97.
23. J.-R. Weng, C.-S. Lin, H.-C. Lai *et. al*. Antiviral activity of Sambucus FormosanaNakai ethanol extract and related phenolic acid constituents against human coronavirus NL63. *Virus Res* **2019**, 273197767.
24. X.-L. Zhang, Y.-S. Guo, C.-H. Wang *et. al*. Phenolic compounds from Origanum vulgare and their antioxidant and antiviral activities. *Food Chemistry* **2014**, 152300-06.
25. Y. Li, Y. Liu, A. Ma *et. al.* In vitro antiviral, anti-inflammatory, and antioxidant activities of the ethanol extract of Mentha piperita L. *Food Science and Biotechnology* **2017**, 26(6), 1675-83.
26. R. Li, R. Narita, H. Nishimura *et. al*. Antiviral Activity of Phenolic Derivatives in Pyroligneous Acid from Hardwood, Softwood, and Bamboo. *ACS Sustainable Chemistry & Engineering* **2018**, 6(1), 119-26.
27. Y. Gao, L. Yan, Y. Huang *et. al.* Structure of the RNA-dependent RNA polymerase from COVID-19 virus. *Science (New York, N.Y.)* **2020**, 368(6492), 779-82.
28. R.N. Kirchdoerfer, A.B. Ward. Structure of the SARS-CoV nsp12 polymerase bound to nsp7 and nsp8 co-factors. *Nature communications* **2019**, 10(1), 2342.
29. T.C. Appleby, J.K. Perry, E. Murakami *et. al.* Viral replication. Structural basis for RNA replication by the hepatitis C virus polymerase. *Science (New York, N.Y.)* **2015**, 347(6223), 771-5.
30. J.A. Rothwell, J. Perez-Jimenez, V. Neveu *et. al.* Phenol-Explorer 3.0: a major update of the Phenol-Explorer database to incorporate data on the effects of food processing on polyphenol content. *Database* **2013**, 2013.
31. S. Kim, J. Chen, T. Cheng *et. al.* PubChem in 2021: new data content and improved web interfaces. *Nucleic acids research* **2021**, 49(D1), D1388-D95.
32. S. Singh, M.F. Sk, A. Sonawane *et. al.* Plant-derived natural polyphenols as potential antiviral drugs against SARS-CoV-2 via RNA-dependent RNA polymerase (RdRp) inhibition: an in-silico analysis. *Journal of Biomolecular Structure and Dynamics* **2020**1-16.
33. C. Lipinski. Lipinski, C.A. Lead- and drug-like compounds: the rule-of-five revolution. Drug Discov. Today Technol. 1, 337-341. *Drug Discovery Today: Technologies* **2004**, 1337-41.
34. B. Jayaram, T. Singh, G. Mukherjee *et. al.* Sanjeevini: a freely accessible web-server for target directed lead molecule discovery. *BMC Bioinformatics* **2012**, 13(17), S7.
35. E.E. Bolton, J. Chen, S. Kim *et. al.* PubChem3D: a new resource for scientists. *J Cheminform* **2011**, 3(1), 32-32.
36. D.E. Pires, T.L. Blundell, D.B. Ascher. pkCSM: Predicting Small-Molecule Pharmacokinetic and Toxicity Properties Using Graph-Based Signatures. *J Med Chem* **2015**, 58(9), 4066-72.
37. D. Rubin, K. Chan-Tack, J. Farley, A. Sherwat. FDA Approval of Remdesivir — A Step in the Right Direction. *New England Journal of Medicine* **2020**, 383(27), 2598-600.
38. C.J. Gordon, E.P. Tchesnokov, J.Y. Feng *et. al.* The antiviral compound remdesivir potently inhibits RNA-dependent RNA polymerase from Middle East respiratory syndrome coronavirus. *J Biol Chem* **2020**, 295(15), 4773-79.
39. J. Ahmad, S. Ikram, F. Ahmad *et. al.* SARS-CoV-2 RNA Dependent RNA polymerase (RdRp) - A drug repurposing study. *Heliyon* **2020**, 6(7), e04502.
40. S.O. Aftab, M.Z. Ghouri, M.U. Masood *et. al.* Analysis of SARS-CoV-2 RNA-dependent RNA polymerase as a potential therapeutic drug target using a computational approach. *Journal of Translational Medicine* **2020**, 18(1), 275.
41. D.E.V. Pires, T.L. Blundell, D.B. Ascher. pkCSM: Predicting Small-Molecule Pharmacokinetic and Toxicity Properties Using Graph-Based Signatures. *J Med Chem* **2015**, 58(9), 4066-72.
42. C. Prakash, A. Kamel, D. Cui *et. al.* Identification of the major human liver cytochrome P450 isoform(s) responsible for the formation of the primary metabolites of ziprasidone and prediction of possible drug interactions. *Br J Clin Pharmacol* **2000**, 49 Suppl 1(Suppl 1), 35S-42S.